Anal. Bioanal. Electrochem., Vol. 13, No. 1, 2021, 67-79

Analytical& Bioanalytical Electrochemistry

www.abechem.com

Full Paper

Effect of Bias Voltage on Corrosion Behavior of Nanostructured TiN Coatings Deposited on Ti-6Al-4V Alloy by CAE-PVD Technique

Mahsa Mirzaei, Arash Fattah-alhosseini,* Hassan Elmkhah, and Kazem Babaei

Department of Materials Engineering, Bu-Ali Sina University, Hamedan 65178-38695, Iran

*Corresponding Author, Tel.: +988138292505; Fax: +988138257400

E-Mail: a.fattah@basu.ac.ir

Received: 20 March 2020 / Received in revised form: 26 July 2020 / Accepted: 8 August 2020 / Published online: 31 August 2021

Abstract- In this study, TiN coatings were deposited on Ti-6Al-4V alloy surface using cathodic arc evaporation (CAE) deposition process at three different bias voltages (-150, -200 and -250 V) applied to the substrate. In this regard, the effect of bias voltage on the microstructure and corrosion behaviour of coatings was studied. The microstructure of the coated specimens was analysed by scanning electron microscopy (SEM), X-ray diffraction (XRD) and atomic force microscopy (AFM). The corrosion behaviour of the coatings was studied by potentiodynamic polarization (PDP) experiments and electrochemical impedance spectroscopy (EIS) in the simulated media. Studies on SEM images showed that formed coatings at bias of -200 V exhibited the least amount of needle like cavities (0.4%) and macroparticles. Studying the effect of bias voltage on the corrosion behaviour of the coatings deposited at three bias voltages showed that the maximum corrosion resistance was obtained at -200 V and this voltage had the least current density in polarization measurements (5.59×10^{-7} A/cm^2). So, it was considered as the optimal bias voltage.

Keywords- TiN nanostructured coating; Ti-6Al-4V; Physical vapor deposition (PVD); Bias voltage; Electrochemical impedance spectroscopy (EIS)

1. INTRODUCTION

Materials such as Ti-6Al-4V alloy are widely used as dental and orthopedic implants due to their superior strength, optimum toughness and low corrosion rate inside the body [1,2].

However, numerous studies have concluded that these properties are not sufficient to use a material as an implant. Although the Ti-6Al-4V alloy has good corrosion resistance, the release of the metallic ions (aluminium, vanadium and titanium) can pose problems in the biocompatibility of this alloy as a result of wear and corrosion. Other problems of using this alloy as an implant in the body are its poor tribological and bioactivity properties [3–5]. Researchers have used different coating methods to improve the different properties of materials. Among the numerous coating deposition methods, the physical vapour deposition (PVD) process is a suitable approach to deposit hard coatings because of have its numerous benefits including high rate of deposition, strong adhesion to the substrate and possibility of coating different implants with complex shapes has attracted much attention [6].

Different PVD methods such as evaporation deposition [7], electron beam [8–10], sputtering deposition [11,12], and CAE deposition [13–19]. Andalibi Fazel et al. evaluated the electrochemical properties of applied TiN single layer and CrN/TiN nanoscale multilayer coatings deposited by CAE method [5]. The negative applied bias voltage to the substrate highly affects the different coating properties. In general, this parameter affects the mechanical behaviour and corrosion of coatings by affecting the crystallite size as well as coating density [20]. The purpose of this study is to investigate the effect of bias voltage on the electrochemical behaviour of TiN nanostructured coating deposited on Ti-6Al-4V substrate using CAE method. The effect of bias voltage on the structure and properties of different coatings is generally attributed to the resputtering phenomenon depending on the ion bombardment [21]. In fact, the presence of microparticles and needle like cavities on the surface of TiN coatings is evident that the distribution and size of these microparticles varies in different voltages. Bias voltage has a direct effect on corrosion resistance. As expected, the uncoated samples had minimal protection against corrosion attacks in comparison to the coated samples. It is interesting to note that there is a strong relationship between the number of microdroplets and the corrosion rate. These droplets appear to have a significant influence on the corrosion behaviour because they have poor adhesion to the coating surface. These defects will form channels for attacking the corrosive solution to the substrate and consequently increase the corrosion rate [21,22].

As mentioned, the amount of micro droplets decreases dramatically due to the effect of secondary sputtering on the optimal substrate bias. Generally, a cavity-free coating gives the substrate better passive behaviour than coatings having a cavity. These defects can weaken the interface of the material and provide routes for the corrosive solution to penetrate, thereby providing a route for discharge of metal ions [23,24]. In order to evaluate the corrosion behaviour of 316 L stainless steel coated with titanium nitride in simulated human body solution, Yuan et al. deposited this coating on the substrate in two methods including CAE and magnetic sputtering and investigated the effect of substrate bias and nitrogen pressure on it. In this study, an increase in corrosion resistance was observed by increasing bias voltage, possibly due to the fact that the increased ion bombardment on the substrate provides a coating with

denser morphology. In fact, for a coating, the ion receives more energy by increasing the negative bias. High-energy ions can refine large droplets and reduce grain size. Due to the poor adhesion force between the drop and the coating, the use of high energy ions results in the removal of loose bonded droplets and therefore improves the coating properties [25].

Studying the electrochemical behavior of Ti-coated 304 stainless steel, Fatah-alhosseini et al. [26] reported that the EIS results showed that the nanostructured coating exhibited superior passive behavior and was even better than annealed Ti. It was also reported in another study [27] that the superior passive behavior of some nanostructured coatings is due to their finer nanocrystalline structure that facilitates the formation of thicker passive protective coatings. In a study to investigate the biocompatibility of TiN coatings and the release of free ions of substrate, a TiN coating was applied to the NiTi alloy. In this study, the number of nickel ions released from the uncoated alloy increased significantly by increasing the immersion time of the samples in the simulator solution, while the number of nickel ions released from the coated TiN alloy changed slightly within 72 hours [28].

Elmkhah et al. [29] applied nanocrystalline TiN coatings to both HIPIMS and DCMS techniques and observed that HIPIMS-TiN coating had a denser columnar nanostructure and higher polarization resistance than DCMS-TiN. This meant the existence of better protective passive layer on its surface. In another study [30] it was found that the duty cycle parameter plays an essential role in the crystal structure, the nucleation and growth mechanism as well as the deposition rate of these coatings. Investigating the effect of bias voltage on electrochemical behavior of TiN nanostructured coatings by the PVD method in simulated body fluid is the purpose of this study.

2. EXPERIMENTAL PROCEDURE

2.1. Coating deposition

Before coating, the specimens were cleaned in acetone and alcohol for 10 minutes by ultrasound and they were finally dried via hot air. To access the cross-section of the coatings and study their microscopic examination, the specimens were put in the holder after cutting and surface preparation based on the figure and they were investigated after hot mount, sanding and accurate polishing. The nanostructured TiN hard coatings investigated in this study were deposited on Ti-6Al-4V substrates by CAE method. Two cathode arc evaporation sources were used for coating. The volume of the chamber was about one cubic meter. The deposition and device conditions are given in Table 1. The device has a negative bias voltage, which can be changed during the coating process. The specimens are placed on a metal stand inside the apparatus housing to which the bias voltage is applied.

Table 1. Coating parameters using cathodic arc in this study

Parameters	Amount
Target material	Titanium (99.6%)
Working pressure (torr)	5×10^{-3}
Current of target evaporation (A)	100
Distance of source to the base metal (cm)	15
Deposition time (min)	60
Parts rotating rate (RPM)	5
Duty cycle	50%
Deposition temperature (^{o} C)	200
Bias voltage (V)	-150, -200, -250

2.2. Coating specifications

To identify the phases in the coated samples, the XRD pattern was obtained using the Philips PW1730 diffractometer with a Cu Kα beam (wavelength equal to 1.54 Å) from 20 to 80 degrees of diffraction angle. Diffraction patterns were analysed using Xpert HighScore software. The JEOL JSM-840A scanning electron microscope at 1000 and 5000 times magnification was used to observe the surface microstructure. NanoScope III atomic force microscope, Digital Instruments USA, was used to study the surface roughness and structure of the coatings. The scanning size was 5 μm, the scanning rate was 2.001 Hz and the data scale was 200 nm.

2.3. Electrochemical tests

To investigate the electrochemical behavior of the coatings deposited by CAE deposition, EIS and polarization tests were performed on the samples. All electrochemical tests were performed on a flat cell having three electrodes including platinum electrode as auxiliary electrode, silver/ silver chloride saturated electrode as reference electrode and sample tested as working electrode. The compounds used to make the SBF solution are presented in Table 2.

In the EIS method, a small range of potential or current is applied to the working electrode in the frequency range of 100 kHz to 10 mHz and the potential or current behavior is investigated. In this method, the electrochemical cell is followed by an equivalent electrical circuit. Elements of the electrical circuit (resistor, capacitor, and inductor) represent the physical, chemical or electrochemical processes occurring inside the cell. Electrochemical tests

were performed using Origa Master. Also, Zview software was used to model and extract the electrochemical impedance curves.

Table 2. Chemical composition of SBF solution used in this article

Reagent	Composition (g/l)
NaCl	8.00
$C_6H_{12}O_6.H_2O$	1.00
$MgCl_2.6H_2O$	0.4
KCl	0.4
$NaHCO_3$	0.35
CaCl2	0.14
$Na_2HPO_4.2H_2O$	0.06
$MgSO_4.7H_2O$	0.06

3. RESULTS AND DISCUSSION

3.1. Microstructural evolutions

As shown in Fig. 1, the patterns shown indicate that different crystalline plates, including (111), (200), (220) and (311), are dominant for all coated samples and The phase composition of the coating mainly comprises TiN. Generally, increasing the bias voltage from -150 to -250 V increases the intensity of the peaks in the crystalline plates and in all coatings the highest peak belongs to the plate (111). However, its intensity is less than other voltages at a voltage of -250 V. This is probably related to the FCC structure of titanium nitride coatings. Increase of bias voltage affects kinetic energy of random particles in substrate surface and the competition between strain energy and surface energy in TiN coatings applied at different bias voltages causes the growth to change. In general, the crystalline orientation of the deposited coatings is significantly influenced by the degree of substrate bias.

From a kinetic point of view, if coatings grow under conditions of relatively high energy ions, they tend to form coatings with open channels. For TiN coatings, the plates (200) contain more open channels than the plates (111). As can be seen in the XRD patterns of the deposited coatings in different bias, the peak intensities (200) for the voltage -250 V are higher than both -150 and -200 V. And these results are completely consistent with the SEM images observed from the surface of the coatings.

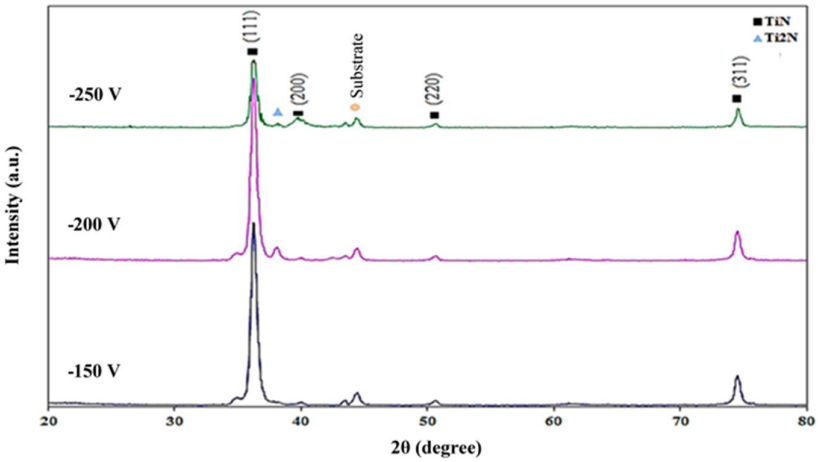

Fig. 1. XRD patterns of deposited coatings at different substrate bias voltages

According to Fig. 2 and irrespective of the bias voltage, small micro droplets of Ti are visible in all three shapes resulting from the melted titanium cathodes. CAE coatings frequently possess defects like macro particles (i.e. metal droplets ejected from the cathode spot) within the whole coating volume and grain boundaries. The coating mechanical damage arises from the occurrence of those defects exposing the substrate that declines the components corrosion resistance in addition to the mechanical strength [31]. These micro droplets cause open cavities. The magnitude of these micro droplets, as is clearly seen in the images, is greater than -200 V at bias voltages of -150 V and -250 V. As mentioned, the substrate temperature increases as the bias voltage increases, in this condition, the particles change their location from the surface and leave their voids in the form of pits and needle like holes. In fact, at -150 V bias voltage due to the high number of micro droplets, a large number of holes are created on the surface of the coating. Increasing the substrate bias voltage to an optimum of -200 V by increasing the substrate temperature contributes to the formation of a dense structure of TiN coating, this is when the microdroplets mentioned which do not have a large number, retaining their surface location after evaporation from the target material and by increasing the temperature and bombarding the substrate with more energetic ions at -250 V, the high temperature combined with the large number of micro droplets causes more of these particles to be removed from the surface and leave holes. The change in the number of droplets at -250 V bias voltage is a function of changes in the energy level.

Fig. 3 shows the atomic force microscope image for all three voltages. The surface of the coated specimens at bias voltage of -150 V indicates that there are some irregularities in the distribution and the existence of large and irregular grains and it seems that the intergranular columnar boundaries are not dense as shown by some cavities near the borders. At a higher bias voltage (Fig. 3b), the grains are more abundant and at the same time smaller and greater surface uniformity is observed. In fact, as the bias voltage increases, the mobility of ions and surface atoms increases, resulting in the formation of dense coatings and lower roughness levels in the coatings. Instead, the

surface morphology of the specimens coated at -250 V bias voltage (Fig. 3c), shows a different pattern. The grains are unevenly distributed and the surface of the coatings represents a lumpy topography formed by relatively loose and larger columns. Generally, increase the roughness at this voltage is due to the bombardment of high-energy ions.

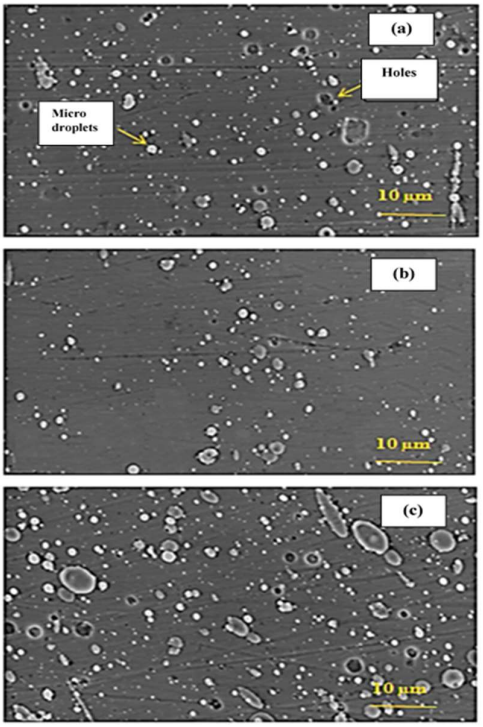

Fig. 2. SEM images of TiN coatings deposited at different bias voltages of the substrate: (a) -150 V, (b) -200 V, and (c) -250 V

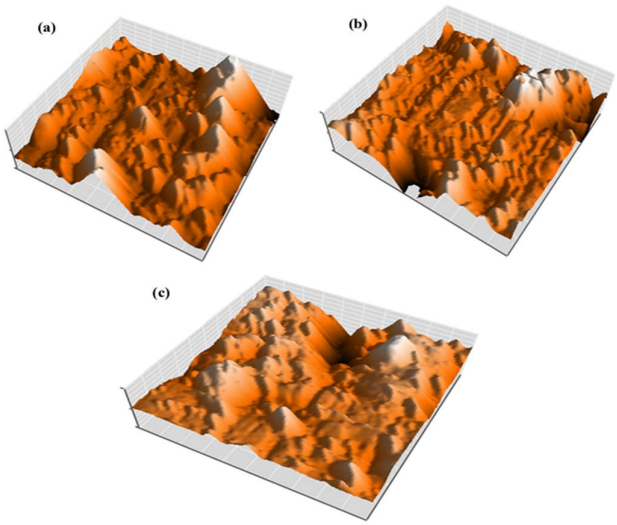

Fig. 3. Three-dimensional AFM images of deposited coatings at voltages of: (a) -150 V, (b) -200 V and (c) -250 V

The numbers for the roughness of titanium nitride coatings as a function of bias voltage are given in Table 3. Increasing the bias voltage from -150 to -200 V will decrease the surface roughness. This decrease is mainly due to the density of the coating material due to ion bombardment. Also, reduction of micro droplets at this voltage is very effective on reducing roughness at this voltage. In general, at lower bias voltages, more energy in the near-surface region increases the atomic mobility to form larger clusters. As the bias voltage increases, this energy is neutralized by random ions. Therefore, greater surface uniformity is obtained, and thus the decreasing trend in the surface roughness parameter is justified by increasing the bias voltage [23].

Table 3. Roughness numbers for TiN coatings applied at different bias voltages

Sample	(Ra)	(Rz)	(Rmax)
-150 V	57.1	396.1	486.6
-200 V	53.2	322.2	458.7
-250 V	60.3	414.9	492.2

3.2. Electrochemical tests

According to reports, the surface corrosion phenomenon initially begins with defects such as cavities and grain boundaries. The corrosive solution is driven through these small channels by the capillary force to the substrate. It is noteworthy that coatings deposited by the CAE are denser and more resistant against corrosion than the other methods [32].

Fig. 4 shows Nyquist and Bode curves obtained by EIS test for Ti-6Al-4V samples and also with coatings applied to this substrate at voltages of -150, -200 and -250 V. Similar Nyquist and Bode plots were reported for TiN single layer and CrN/TiN nanoscale multilayer coatings deposited by CAE method in Hank's solution [5]. These graphs are plotted based on real and imaginary impedance data. The Nyquist diagram (Fig. 4(a)) shows that the coatings consist of two capacitive loops, indicating the presence of two layers in the coating structure. The loop created at high frequencies corresponds to the outer porous layer and at low frequencies represents the inner compact layer or the common segment between the coating and the substrate. According to the Bode curve (Fig. 4(b)), the impedance (Z) that shows corrosion resistance for uncoated specimens and coated ones at voltages of -250, -150 and -200 V increases respectively in the low-frequency range that indicates the coated samples have better corrosion behaviour in these conditions than the uncoated ones and the coated sample at -200 V has the highest impedance and best corrosion behaviour in the simulated body fluid.

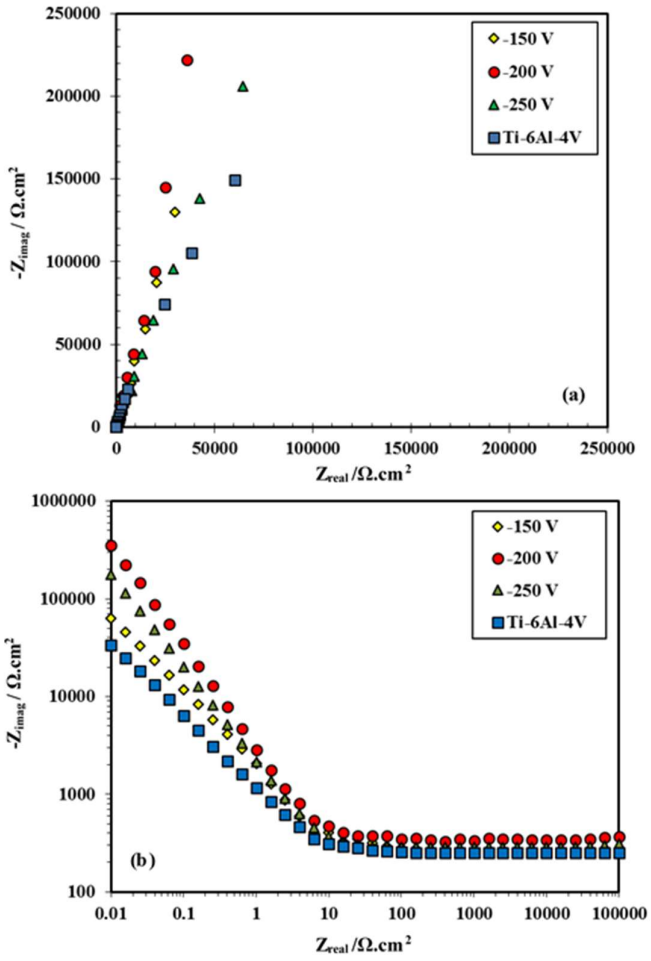

Fig. 4. (a) Nyquist, and (b) Bode curves Ti-6Al-4V samples coated under different bias voltages in SBF solution

To model the electrochemical behaviour of the coatings, the proposed equivalent circuit of Fig. 5 was used. In this circuit, R_S is the solution resistance between coating surface and reference electrode, R_1 and CPE_1 are related to the resistance and the constant phase element (CPE) of the outer porous layer, R_2 and CPE_2 are related to the resistance and the CPE of the inner porous layer, respectively. Table 4 shows the results of modelling the obtained data from the equivalent impedance spectroscopy. It is clear that inner layer resistance for all of the coatings is much greater than the outer layer resistance. This indicates that the dense inner layer plays an important role in protecting the coatings against corrosion. In addition, the resistances of the inner and outer layers increase as the substrate bias voltage increases from -150 V to -200 V. But as the voltage increases to -250 V, the resistance of the inner and outer layers decreases. As a result, the coated sample at -200 V has the highest inner layer resistance and therefore the best corrosion behaviour.

Table 4. Data extracted from the proposed equivalent circuit

Sample	R_{inner} (MΩ.cm^2)	R_{outer} (kΩ.cm^2)	$R_{solution}$ (Ω.cm^2)
Ti-6Al-4V	0.28	0.98	414
- 150 V	0.97	1.8	419
- 200 V	1.35	2.2	431
- 250 V	0.78	1.1	412

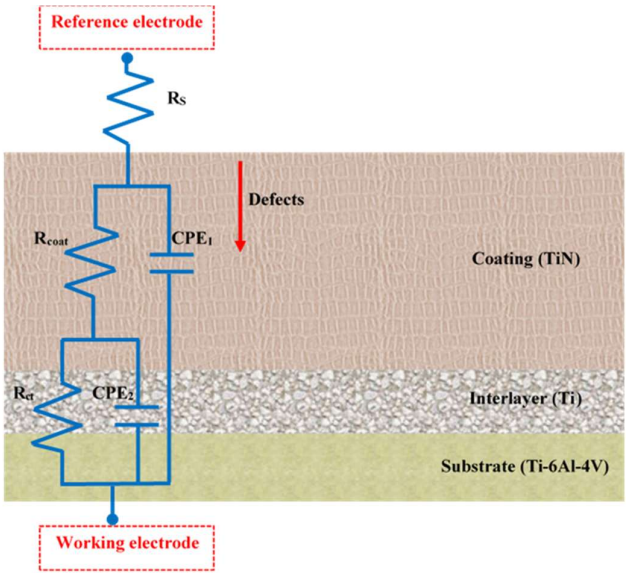

Fig. 5. Proposed equivalent electrical circuit for modelling corrosion behaviour of coatings

PDP test was used to find out the effect of increasing bias voltage on the corrosion behaviour of the coatings. The curves of the PDP test of the samples are shown in Fig. 6 after 48 hours immersion in Ringer's solution. Similar PDP plots were reported for TiN single layer and CrN/TiN multilayer coatings deposited by CAE method in Hank's solution [5]. For all of these three voltages, the same electrochemical behaviour is observed. The PDP curves shift to higher potential and lower corrosion current density by increasing the bias voltage from-150 to -200 V, while both of potential and corrosion current density decrease with increasing bias voltage to -250 V. The corrosion current densities obtained from plots of PDP using the method of Tafel linear extrapolation [33–36]. The minimum and maximum current densities were obtained for the voltages of -200 and -250 V, with values of 5.59×10^{-7} A/cm^2 and 1.23×10^{-5} A/cm^2, respectively. Generally, a no-cavity coating gives the substrate better passive behaviour than coatings with cavities. These defects can weaken the interface of the material and provide

routes for penetration of the corrosive liquid, thereby providing a route for the discharging metallic ions. Some obtained electrochemical data from the PDP curve such as corrosion potential (E_{corr}) and corrosion current density (i_{corr}) are presented in Table 5.

Table 5. Electrochemical data extracted from the potentiodynamic polarization curve for Ti-6Al-4V alloy coated at different bias voltages

Sample	-150 V	-200 V	-250 V
E_{corr} ($V_{Ag/AgCl}$)	-0.379	-0.357	-0.469
i_{corr} (µA.cm^{-2})	3.23	5.59	12.3

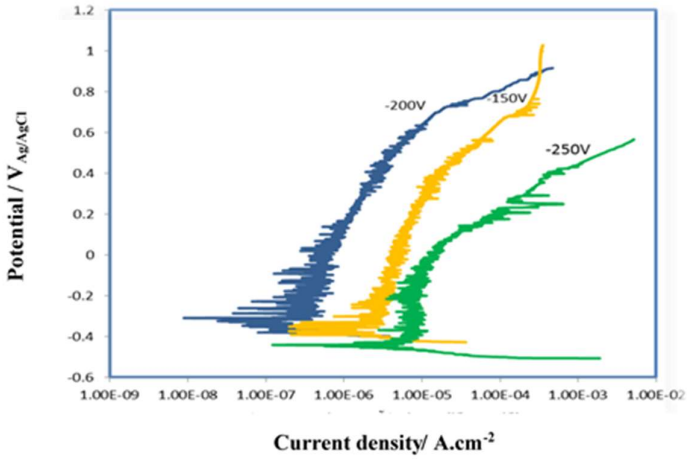

Fig. 6. Polarization curves of Ti-6Al-4V samples coated at different bias voltages

4. CONCLUSION

The XRD patterns examination of the samples showed that different crystalline planes, including (111), (200), (220) and (311), were dominant for all of the coated samples and the coating phase composition mainly comprises TiN. In all of the coatings, the strongest peak belongs to the plate (111) and the peak intensity (200) at the voltage of -250 V is higher than the other voltages. Moreover, studying SEM images of deposited coatings in different substrate biases showed that formed coatings at bias voltage of -200 and -250 V, provided the minimum and maximum amount of needle like cavities and micro droplets, respectively. Also, surface roughness studies and observations of atomic force microscopy images of the coatings at the three bias voltages showed a decrease in roughness at -200 V bias voltage and an increase in surface uniformity and smaller grain size at this voltage. Studying the effect of bias voltage on

the corrosion behaviour of the deposited coatings at the three bias voltages studied showed that the maximum hardness values of the inner and outer layers were obtained at -200 V. Also, this voltage was considered as the optimum voltage in the polarization measurements with the lowest current density value (5.59×10^{-7} A/cm^2).

REFERENCES

[1] S. A. Naghibi, K. Raeissi, and M. H. Fathi, Mater. Chem. Phys. 148 (2014) 614.
[2] J. Fojt, Appl. Surf. Sci. 262 (2012) 163.
[3] M. A. Khan, R. L. Williams, and D. F. Williams, Biomaterials 20 (1999) 631.
[4] N. Sahib Mansoor, A. Fattah-alhosseini, A. Shishehian, and H. Elmkahah, Mater. Res. Express. 6 (2019) 056421.
[5] Z. Andalibi Fazel, H. Elmkhah, A. Fattah-alhosseini, K. Babaei, and M. Meghdari, J. Asian Ceram. Soc. 8 (2020) 510.
[6] G. S. Kaliaraj, M. Bavanilathamuthiah, K. Kirubaharan, D. Ramachandran, T. Dharini, K. Viswanathan, and V. Vishwakarma, Surf. Coatings Technol. 307 (2016) 227.
[7] H. Elmkhah, A. Fattah-alhosseini, K. Babaei, A. Abdollah-Zadeh, and F. Mahboubi, J. Asian Ceram. Soc. 8 (2020) 72.
[8] C. Metzner, K. Goedicke, G. Hoetzsch, B. Scheffel, and J.-P. Heinss, Surf. Coatings Technol. 94–95 (1997) 663.
[9] B. Scheffel, C. Metzner, K. Goedicke, J.-P. Heinss, and O. Zywitzki, Surf. Coatings Technol. 120–121 (1999) 718.
[10] B. B. M., and V. M. K., J. Taibah Univ. Sci. 11 (2017) 1232.
[11] P. Klein, B. Gottwald, T. Frauenheim, C. Köhler, and A. Gemmler, Surf. Coatings Technol. 200 (2005) 1600.
[12] N. S. Lawand, P. J. French, J. J. Briaire, and J. H. M. Frijns, Procedia Eng. 47 (2012) 726.
[13] H. Randhawa, and P. C. Johnson, Surf. Coatings Technol. 31 (1987) 303.
[14] P. A. Lindfors, W. M. Mularie, and G. K. Wehner, Surf. Coatings Technol. 29 (1986) 275.
[15] G. T. P. Azar, C. Yelkarasi, and M. Ürgen, Surf. Coatings Technol. 322 (2017) 211.
[16] P. Mohamadian Samim, A. Fattah-Alhosseini, H. Elmkhah, and O. Imantalab, J. Asian Ceram. Soc. 8 (2020) 460.
[17] P. Mohamadian Samim, A. Fattah-alhosseini, H. Elmkhah, and O. Imantalab, Mater. Res. Express. 6 (2019) 126426.
[18] K. Jokar, H. Elmkhah, A. Fattah-alhosseini, K. Babaei, and A. Zolriasatein, Mater. Res. Express. 6 (2019) 116426.

[19] N. Sahib Mansoor, A. Fattah-alhosseini, H. Elmkhah, and A. Shishehian, Mater. Res. Express. 6 (2020) 126433.
[20] W. Olbrich, J. Fessmann, G. Kampschulte, and J. Ebberink, Surf. Coatings Technol. 49 (1991) 258.
[21] A. Shah, S. Izman, M. R. Abdul Kadir, H. Mas-Ayu, M. Anwar, and A. B. Ma'aram, Adv. Mater. Res. 845 (2013) 436.
[22] F. R. Attarzadeh, H. Elmkhah, and A. Fattah-alhosseini, Metall. Mater. Trans. B. 48 (2017) 227.
[23] N. D. Nam, J. G. Kim, and W. -S. Hwang, Thin Solid Films. 517 (2009) 4772.
[24] N. Sahib Mansoor, A. Fattah-alhosseini, A. Shishehian, and H. Elmkhah, Anal. Bioanal. Electrochem. 11 (2019) 304.
[25] L. Yuan, Y. Gao, W. Zhang, C. L. Wang, Z. K. Ma, and H. W. Cai, Adv. Mater. Res. 399–401 (2011) 1898.
[26] A. Fattah-alhosseini, H. Elmkhah, and F. R. Attarzadeh, J. Mater. Eng. Perform. 26 (2017) 1792.
[27] A. Fattah-alhosseini, H. Elmkhah, G. Ansari, F. Attarzadeh, and O. Imantalab, J. Alloys Compd. 739 (2018) 918.
[28] Z. Lifeng, H. Yan, Y. Dayun, L. Xiaoying, X. Tingfei, Z. Deyuan, H. Ying, and Y. Jinfeng, Biomed. Mater. 6 (2011) 025012.
[29] H. Elmkhah, F. Attarzadeh, A. Fattah-alhosseini, and K. H. Kim, J. Alloys Compd. 735 (2018) 422.
[30] H. Elmkhah, A. Abdollah-zadeh, F. Mahboubi, A. R. S. Rouhaghdam, and A. Fattah-alhosseini, J. Alloys Compd. 711 (2017) 530.
[31] N. Sahib Mansoor, A. Fattah-alhosseini, H. Elmkhah, and A. Shishehian, J. Asian Ceram. Soc. (2020) https://doi.org/10.1080/21870764.2020.1776915.
[32] X. Tian, R. K. Y. Fu, and P. K. Chu, J. Vac. Sci. Technol. A 20 (2002) 160.
[33] G.T. Burstein, Corros. Sci. 47 (2005) 2858.
[34] E. McCafferty, Corros. Sci. 47 (2005) 3202.
[35] A. Fattah-alhosseini, M. Vakili-Azghandi, M. Sheikhi, and M. K. Keshavarz, J. Alloys Compd. 704 (2017) 499.
[36] S. Vafaeian, A. Fattah-alhosseini, M. K. Keshavarz, Y. Mazaheri, J. Alloys Compd. 677 (2016) 42.